Experimental study on thermal conductivity of paraffin-based shape-stabilized phase change material with hybrid carbon nano-additives

Y. Qu [a], S. Wang [a], D. Zhou [b] ,Y. Tian [c]

[a] School of Chemical Engineering, China University of Petroleum, Qingdao 266580, China
[b] Centre for Renewable Energy Systems Technologies (CREST),
Wolfson School of Mechanical, Electrical and Manufacturing Engineering,
Loughborough University, Leicestershire, LE11 3TU, UK
[c] School of Engineering and Sustainable Development
De Montfort University, Leicestershire, LE1 9BH, UK

Abstract: Thermal energy storage with Phase Change Materials (PCMs) is one of the most potential technologies for energy storage. However the low thermal conductivity of PCMs reduces the heat exchange rate during melting and solidification cycles. This paper studied the effects of two hybrid Carbon Nano-additives (CNs) fillers, that is, Expanded Graphite-Multi-walled Carbon Nano-tube (EG-MWCNT) and Expanded Graphite-Carbon Nano-fiber (EG-CNF), on the thermal conductivity of Paraffin-HDPE SSPCM. From the viewpoints of synergistic thermal enhancement effect and the interfacial thermal resistance, the principle of enhancing thermal conductivity of Paraffin-HDPE/EG-MWCNT and Paraffin-HDPE/EG-CNF composite PCMs was analyzed. A modified Maxwell-Garnett model with a synergy factor η was proposed, which found excellent agreement between model prediction and the experimental data. Compared with the 5wt% loading of single CN additive EG, the thermal conductivities of hybrid CNs fillers (EG-MWCNT and EG-CNF) Paraffin-HDPE SSPCM had increased by 60% and 21.2% respectively. Within the scope of mass ratios of hybrid CNs fillers in this paper, Paraffin-HDPE/EG-MWCNT composite PCM exhibited superior performance than Paraffin-HDPE/EG-CNF in thermal conductivity with the optimal mass ratio of EG and MWCNT being 4:1.

Keyword: Shape-stabilized PCM; thermal conductivity; synergistic effect; hybrid carbon nano-additives

Please cite as:
Y. Qu, S. Wang, D. Zhou, **Y. Tian**, “Experimental Study on Thermal Conductivity of Paraffin-Based Shape-Stabilized Phase Change Material with Hybrid Carbon Nano-Additives”, *Renewable Energy* 146, 2020, pp. 2637–2645, https://doi.org/10.1016/j.renene.2019.08.098

Nomenclature

d	diameter	m
De	deviation	%
H_m	latent heat	kJ/kg
k	thermal conductivity	W/(m·K)
l	length	m
r	radius	m
R	radius of phase transition	m
R_{Bd}	interface thermal resistance	m^2K/W
s	area fraction	%
t	time	s
T_0	uniform temperature	°C
T_∞	ambient temperature	°C
T_m	phase change temperature	°C
V	volume fraction	%
w	mass fraction	%
Acronyms		
BN	boron nitride	
CBT	cyclic butylene terephthalate	
CN	carbon nano-additives	
CNF	carbon nano-fibers	
EG	expanded graphite	
EGP	expanded graphite platelets	
EVA	ethylene vinyl acetate	
GF	grapheme foam	
GNP	graphite nanoplatelets	
GO	graphene oxide	
HDPE	high density polyethylene	
LDPE	low density polyethylene	
MFR	melt mass-flow rate	
MGF	multilayer graphene	
MGP	multi-graphene platelets	
MPCM	microencapsulated phase change materials	
MWCNT	multi-walled carbon nanotubes	
PCF	pitch-based carbon fibers	
PDMS	polydimethylsiloxane	
PEG	polyethylene glycol	
SBS	styrene-butadiene-styren	
SSPCM	shape-stabilized phase change materials	
SWCNT	single-walled carbon nano-tubes	
Greek letter		
α	dimensionless parameter	
ζ	radius of the phase transition position	m
η	synergy factor	
ρ	density	g/cm^3
Subscripts		

c	composite material
f	freezing
m	matrix material
p	particle

1 Introduction

Thermal energy storage (TES) with Phase Change Materials (PCMs) can effectively utilize the intermittent heat source, especially solar energy. Incorporating PCMs into building envelops can passively use solar energy to largely keep the room temperature within a thermal comfort range and in turn to reduce energy consumed by heating and cooling. The most potential materials are paraffin-based PCMs due to their suitable melting temperatures (18 °C to 30 °C), negligible super-cooling effect, low cost and excellent thermal and chemical stabilities. However, the disadvantage of low thermal conductivity (with an average of 0.2 W/(m·K)) reduces the heat transfer rate during the melting and solidification cycles. Several methods can be used to enhance the thermal conductivity of paraffin, such as using extended fins in a heat storage system, embedding porous matrices in PCMs (such as metal foams, porous graphite foams and ceramic honeycombs) [1], incorporation of high thermal conductivity fillers (such as carbon nano-additives or metal nano-particles) and PCM microencapsulation.

Many investigations focused on the effects of adding carbon nano-additives (CNs) to paraffin-based composite PCMs due to their excellent thermal conductivities and low densities. The four most studied CNs in paraffin were expanded graphite (EG), carbon nano-fibers (CNFs), exfoliated graphite nanoplatelets (xGNP) and carbon nano-tubes (CNTs) including SWCNTs (Single-walled Carbon Nano-tubes) and MWCNT (Multi-walled Carbon Nano-tubes), the microstructures of which are shown in Fig. 1. From the structure dimensions, GNP is of 2D planar type while CNF and CNT are of 1D tubular type, and EG is of worm-like porous structure. The achievements regarding the thermal conductivity and latent heat enhancement in PCMs/CNs composites were summarized by Amaral et al. [2]. Among all types of CNs, GNP and EG have the better beneficial effect in thermal conductivity enhancement due to the 2D planar structure of GNP and the worm-like structure of EG by decreasing the filler/matrix interfacial thermal resistance and creating more heat conduction links. However, GNP is prone to aggregation due to the lamellar structure and thereby limits the further enhancement of heat conduction, while EG not only increases the thermal conductivity of PCM and enhances the shape stabilization through retaining the liquid wax by capillary forces formed in the porous structure [3], but also improves the flame retardant properties through the generation of carbonaceous char residue in the condensed phase [4]. Therefore EG was selected in the current study to form the CNs complex with two kinds of 1D structure CNs, which are MWCNT and CNF.

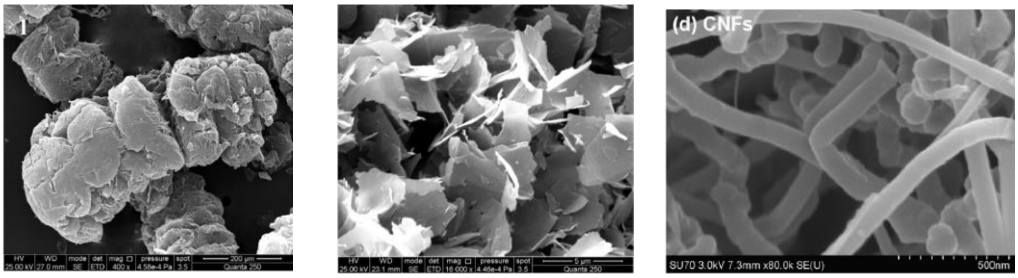

(a) EG [5]　（b）xGnP [5]　（c）CNF [6]

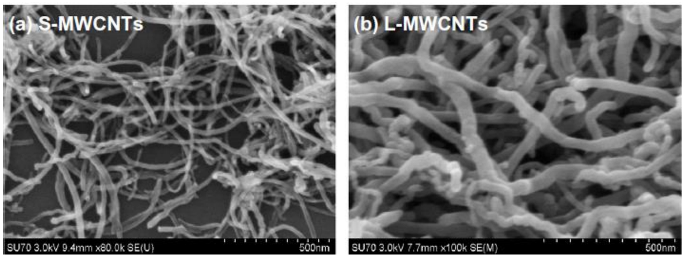

（d）CNTs [6]

Fig. 1 SEM of main CN additives in paraffin

It was not clear whether the thermal conductivity enhancement depends on the type of CNs, the dispersion of CNs into the PCM matrix, intermolecular forces or other reasons [2]. Moreover, most previous works focused on the thermal conductivity enhancement of PCM by single CN, with little discussion on the synergistic effect of multiple hybrid fillers. Several research groups reported synergistic effect in the thermal conductivity enhancement of non-PCM composites by using different microstructure hybrid fillers, such as Multi-graphene Platelets(MGPs)/MWCNT fillers into epoxy [7], Graphene-nanoplatelets (GNPs)/Pitch-based Carbon Fibers (PCFs) fillers into the polymerized Cyclic Butylene Terephthalate (pCBT) [8], GNP/MWCNT fillers into the polycarbonate matrix [9], Multilayer Graphene Flakes (MGFs)/Graphene Foam (GF) fillers into the flexible polymer composites Polydimethylsiloxane (PDMS) [10].

With regards to the synergistic effect on the thermal conductivity enhancement of PCM composites by using hybrid fillers, very little research has been carried out. Tian et al. [11] investigated EG/CF-filled paraffin/Ethylene Vinyl Acetate (EVA) SSPCM with EVA instead of HDPE as the supporting material and with the paraffin of a high phase change temperature (T_m = 50.45°C). The significantly synergistic enhancement to thermal conductivity of FSPCMs was obtained by using CF and EG. Liu and Yang [12] studied expanded graphite platelets (EGP)/MWCNT-filled SSPCM based on paraffin, HDPE, and styrene-butadiene-styrene (SBS) copolymer. They found 9wt.% of EGP and MWCNT increased the thermal conductivity of SSPCM by 246% and 159% respectively. Zou et al. [13] studied MWCNT/graphene filled composite PCM but did not mention the shape stability. Previous works focused on verifying and confirming the synergistic effect ability of enhancing the thermal conductivity of PCM, but rarely studied the mechanism of synergistic effect on the thermal conductivity of PCMs, lacking research in comparing the effects of different combinations of 3D and 1D microstructure CN fillers.

Table 1 The prediction models of thermal conductivity of composite materials

Models	Equation	Application	Refs
Kingery model	$k_c = s_m k_m + s_p k_p$	The first phase is continuous and the second phase is isolated spherules.	[14]
Maxwell-Eucken model	$k_c = \frac{2k_m + k_p + 2V_p\left(k_p - k_m\right)}{k_m + k_p - V_p\left(k_p - k_m\right)} \cdot k_m$	The continuous phase is the dispersed spherical particles, taking into account of the volume fraction of particles.	[15]
Maxwell-Garnett model	$k_c = \frac{\left[k_p\left(1+2\alpha\right)+2k_m\right]+2V_p\left[k_p(1-\alpha)-k_m\right]}{\left[k_p\left(1+2\alpha\right)+2k_m\right]-V_p\left[k_p(1-\alpha)-k_m\right]} \cdot k_m$	Considering the volume fraction of particles, and the size and shape factor of particles are not considered	[16]
Bruggeman model	$(1-V_p) = (\frac{k_c}{k_m})^{(1+2\alpha)/\left[\frac{k_c - k_p(1-\alpha)}{k_m - k_p(1-\alpha)}\right]^{3/(1-\alpha)}}$	Considering the volume fraction of particles, and the change of particle geometry and mixing process is not considered.	[14]
EMT model	$k_c = \frac{3+2V_{p,1}(k_p/k_m)+6V_{p,2}}{3-(V_{p,1}+3V_{p,2})}$	Considering the volume fraction of the continuous phase and particles.	[18]

As composite PCMs belong to heterogeneous component mixing system, there is no theoretical model that can accurately predict their thermal conductivities. There were a large number of studies on the thermal conductivity model of composite materials, such as the Kingery model [14], the Maxwell-Eucken model [15], the Maxwell-Garnett model [16], the Bruggeman model [14] and the improved EMT model [18], which predict the effective thermal conductivity based on the thermal conductivity of the components, volume fraction and shape factor. The formulae for predicting the effective thermal conductivity of the above-mentioned models are shown in Table 1. When using these models, it is usually assumed that the composite matrix is a continuous phase and the thermal conductive fillers are particles with a certain shape dispersed in the matrix. However, these prediction models only involve one single dispersed phase and two hybrid fillers as disperse phased are not considered.

In the current paper, paraffin-based SSPCM for solar building applications with enhanced thermal conductivity was investigated. In order to use the minimum high density polyethylene (HDPE) to obtain the double effects of minimizing the thermal degradation whilst avoiding the leakage of Paraffin-HDPE SSPCMs, the HDPE mass fraction of 17% to 29% was chosen. With paraffin-HDPE matrix regarded as the continuous phase and EG/MWCNT/CNF thermal conductive fillers regarded as the dispersed phase, an improved formula for calculating synergistic thermal conductivity was obtained and verified by experiment. The synergistic effects of thermal conductivity enhancement for two kinds of hybrid CNs fillers, such as EG-MWCNT and EG-CNF, in Paraffin-HDPE SSPCMs were studied theoretically.

2 Experiment

2.1 Materials

The specifications and suppliers of materials used in the test are listed in Table 2. Octadecane with a melting point of 28 °C was selected as the PCM and high density polyethylene (HDPE) with high strength was applied as the shaping material. Three types of CNs: expanded graphite (EG), multi walled carbon nanotubes (MWCNT) and carbon nanofibers (CNF) were used to enhance the thermal conductivity of PCM.

2.2 Sample preparation

The preparation process of the three composite PCMs is shown in Fig. 2 with their composition details given in Table 3. In preparation of Paraffin-HDPE SSPCM samples, paraffin and HDPE were firstly melted in an oil bath at 180 °C and meanwhile blended by a cantilever agitator at a screw speed of 1500 rpm (revolutions per minute) for 30 min. After uniform mixing, the mixed liquid was injected into a stainless steel mold and repressed, which then cooled down to the room temperature. Finally the samples were dried in an air-dry oven and each sample weighed 2 g. Five mass fractions of HDPE, that is, 17%, 20%, 23%, 26% and 29% were prepared and tested to determine the reasonable mass fraction of HDPE in the composite PCMs. The preparation processes of Paraffin-

HDPE/EG-MWCNT and Paraffin-HDPE/EG-CNF composite PCMs were the same as those of Paraffin-HDPE preparation, with an extra step of adding EG-CNF and EG-MWCNT hybrid fillers into liquid Paraffin-HDPE for continuous blending of 30 min. The total mass fraction of thermal conductive fillers was 5% in which the mass ratios of EG-CNF and EG-MWCNT were 5:0, 4:1, 3:2, 1:1, 0:5, respectively, with each sample being 22 g.

Table 2 Specifications and suppliers of the materials used

Materials	Purity (%)	ρ (g/cm^3)	k (W/(m·K))	Features	Supply
Octadecane	98	0.7768	0.25	T_m: 28 °C H_m: 243.5 kJ/kg	Sinopharm Chemical Reagent Co.,Ltd
HDPE	98	0.94	0.4	T_m:130 °C MFR:2.5 g/min	China Petroleum & Chemical Co.,Ltd
EG	98	0.035	3000	Granularity:75μm Expansion ratio: 350 ml/g	Qingdao Hengrunda Graphene Co.,Ltd
MWCNT	98	0.094	1950	External diameter: < 8 nm Length: 10-20 μm	Chengdu Organic Chemical Co.,Ltd
CNF	90	0.035	1150	Diameter: 200-600 nm Length: 5-50 μm	Suzhou Tanfeng Graphene Technology Co., Ltd.

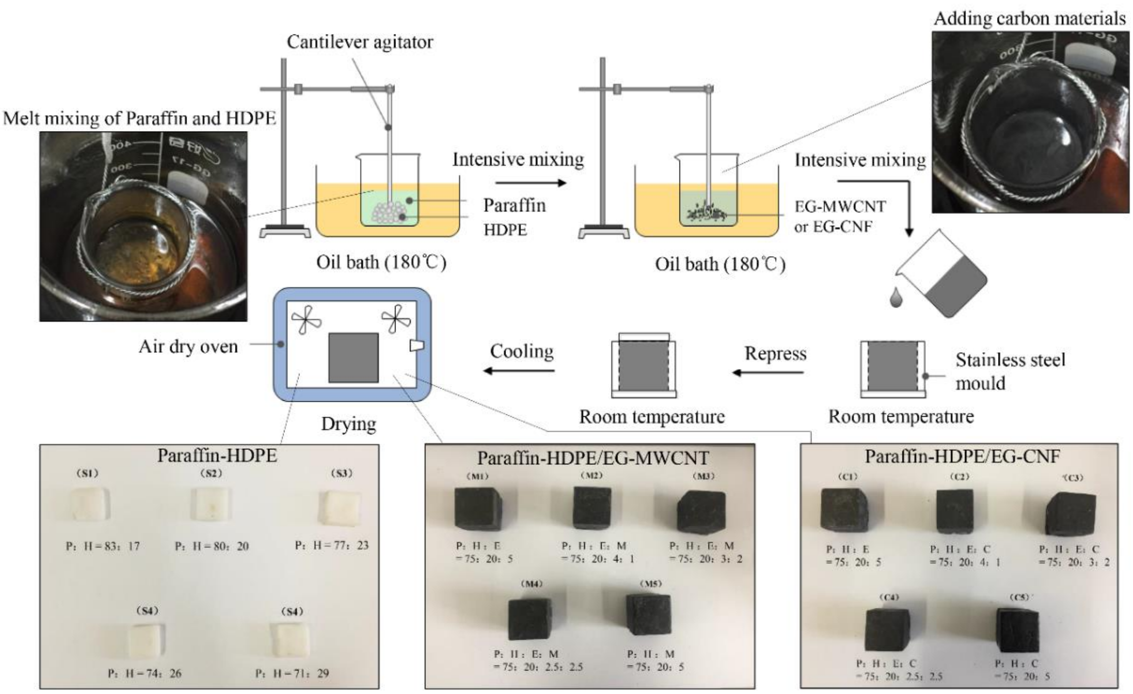

Fig. 2. Schematic diagram of the composite PCMs preparation process

Table 3 Compositions of Paraffin-HDPE, Paraffin-HDPE/EG-MWCNT and Paraffin-HDPE/EG-

CNF

Samples	No.	Paraffin (wt.%)	HDPE (wt.%)	Thermal conductive fillers (wt.%)		
				EG	MWCNT	CNF
Paraffin -HDPE	S1	83	17			
	S2	80	20			
	S3	77	23			
	S4	74	26			
	S5	71	29			
Paraffin -HDPE /EG-MWCNT	M1	75	20	5	0	
	M2	75	20	4	1	
	M3	75	20	3	2	
	M4	75	20	2.5	2.5	
	M5	75	20	0	5	
Paraffin -HDPE /EG-CNF	C1	75	20	5		0
	C2	75	20	4		1
	C3	75	20	3		2
	C4	75	20	2.5		2.5
	C5	75	20	0		5

2.3 Thermal conductivity tested by the T-history method

The thermal conductivity (k) of composite PCMs was derived by the T-history method presented by Zhang et al [17]. The T-history method enables to obtain melting point, latent heat, specific heat, thermal conductivity of several PCM samples simultaneously. The experimental setup is shown in Fig. 3. Firstly, 2/3 volume of test tubes were filled with prepared composite PCM and one tube was filled with the reference material of water due to its well-known thermophysical properties. The filling mass of each sample was 8~10 g depending on the filling material. Then the tubes with samples and reference material were preheated in a thermostatic water bath to a uniform temperature of T_0 = 65 °C which is above the paraffin melting temperature T_m. Finally, the test tubes were simultaneously subjected to the ambient temperature T_∞. Before the test, the pre-experiments were carried out until the sample were stable. In the T-history test, each sample was tested for three times and the curves of temperature history (T versus. t) were recorded during cooling process for each time. The average value of the three times was used in the modelling.

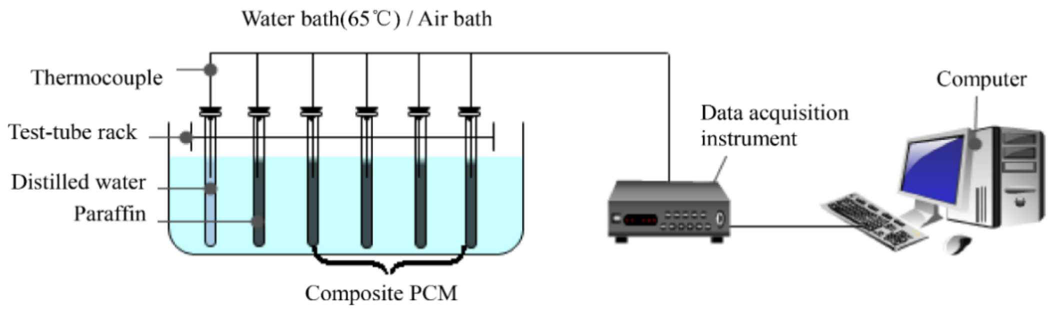

Fig. 3. Experimental device diagram of the T-history method

Here the T-t curve in solidification process was used to analysis the heat conduction coefficient of PCM. The tubes with liquid PCM samples with the initial temperature T_0 ($T_0 > T_m$) was put into a thermostatic water bath with T_∞ ($T_\infty < T_m - \Delta T$). As the convective heat transfer coefficient of the test tubes and the thermostatic water bath was not negligible, the traditional lumped parameter method cannot be adopted. To solve the thermal conductivity of PCM by the T-history method, it is necessary to assume: (1) the phase transition process is approximately quasi-stable; (2) the physical properties of the PCM are constant; (3) the thermal resistance of the test tube wall is negligible; (4) the length-diameter ratio of the test tube is more than 10 [20].

The heat conduction differential equation in a cylindrical-coordinate system in the test tube is approximately described in Eq. (1).

$$\frac{1}{r}\frac{\partial}{\partial r}\left(r\frac{\partial T}{\partial r}\right)=\frac{1}{\alpha}\frac{\partial T}{\partial t}\left(\zeta < r < R, t > 0\right) \tag{1}$$

The boundary condition is presented in Eq. (2).

$$t > 0,\ r = R, T = T_\infty \tag{2}$$

The initial condition is presented in Eq. (3).

$$t = 0,\ \zeta = R, T = T_m \tag{3}$$

The solid-liquid interface conditions are presented in Eqs. (4.1) and (4.2).

$$T\left(r=\zeta\right)=T_m \tag{4.1}$$

$$k\left.\frac{\partial T}{\partial r}\right|_{r=\zeta}=\rho H_m\cdot\frac{d\zeta}{dt}\quad\left(r=\zeta\right) \tag{4.2}$$

where k is the thermal conductivity of solid PCM (W/(m·K)), ρ is the density of composite PCM (kg/m^3) and $\rho=(\rho_1 V_1+\rho_2 V_2)/(V_1+V_2)$ (Subscripts 1, 2 represent the compositions in composite PCM), H_m is the latent heat of PCM (kJ/kg).

The temperature equation at the quasi-steady assumption is described Eq. (5).

$$T(r)= C_1 \ln r + C_2 \tag{5}$$

where C_1 and C_2 are constants.

Substituting Eqs. (2),(3) ,(4.1), and (4.2) into Eq. (5) leads to Eqs. (6.1) and (6.2).

$$T_{\infty} = C_1 \ln R + C_2 \tag{6.1}$$

$$T_{\infty} = C_1 \ln z + C_2 \tag{6.2}$$

Solving the Eqs. (6.1) and (6.2) simultaneously, Eq. (7.1) and Eq. (7.2) can be obtained.

$$C_1 = \frac{T_{\infty} - T_m}{\ln(R/z)} \tag{7.1}$$

$$C_2 = T_m - \frac{(T_m - T_z)?\ln z}{\ln(R/z)} \tag{7.2}$$

Substituting Eqs. (7.1) and (7.2) back into Eq. (5) leads to Eq. (8).

$$T(r) = (T_{\infty} - T_m)\frac{\ln(r/z)}{\ln(R/z)} + T_m \tag{8}$$

Substituting Eq. (6) into the solid-liquid interface conditions Eq. (4.1) and (4.2) leads to Eq. (9).

$$\frac{k}{\rho H_m} dt = \frac{\zeta \ln(R/\zeta)}{T_\infty - T_m} d\zeta \tag{9}$$

Integrating variable t from 0 to t_f for the left hand side of Eq. (9) and integrating variable ζ from 0 to R for the right hand side of Eq. (9), the solidification time t_f of PCM can be obtained.

$$t_f = \frac{\rho H_m R^2}{4k(T_m - T_\infty)} \tag{10}$$

The equation for solving the thermal conductivity k of the solid composite PCM can be obtained in Eq. (11).

$$k = \frac{\rho H_m R^2}{4t_f (T_m - T_\infty)} \tag{11}$$

Eq. (11) also applied to the thermal conductivity calculation of liquid composite PCM. The calculation of PCM fusion heat H_m can follow the method from [20].

2.4 Uncertainty analysis

For the directly measured quantity x_i, the uncertainty is calculated by the Bethel Eq. (12)-(13).

$$\hat{\sigma} = \sqrt{\frac{1}{n-1}\sum_{i=1}^{n}(x_i - \bar{x})^2} \tag{12}$$

$$\bar{x} = \frac{1}{n}\sum_{i=1}^{n} x_i \tag{13}$$

For the indirectly measured quantity $\boldsymbol{Y}_i$, Eq. (14)-(17) is used.

$$\Delta Y = \frac{\partial F}{\partial x_1}\Delta x_1 + \frac{\partial F}{\partial x_2}\Delta x_2 + \ldots\ldots + \frac{\partial F}{\partial x_m}\Delta x_m \tag{14}$$

$$\begin{aligned}(\Delta Y)^2 &= (\frac{\partial F}{\partial x_1})^2(\Delta x_1)^2 + (\frac{\partial F}{\partial x_2})^2(\Delta x_2)^2 + \ldots\ldots + (\frac{\partial F}{\partial x_m})^2(\Delta x_m)^2 \\ &+2\frac{\partial F}{\partial x_1}\frac{\partial F}{\partial x_2}\Delta x_1\Delta x_2 + 2\frac{\partial F}{\partial x_1}\frac{\partial F}{\partial x_3}\Delta x_1\Delta x_3 + \ldots\ldots\end{aligned} \tag{15}$$

$$\sigma_y^2 = (\frac{\partial F}{\partial x_1})^2\sigma_1^2 + (\frac{\partial F}{\partial x_2})^2\sigma_2^2 + \ldots\ldots + (\frac{\partial F}{\partial x_m})^2\sigma_m^2 \tag{16}$$

$$\sigma_y = \sqrt{\alpha_1{}^2\sigma_1{}^2 + \alpha_2{}^2\sigma_2{}^2 + \ldots\ldots + \alpha_m{}^2\sigma_m{}^2} = \sqrt{\sum_{i=1}^{m}\alpha_i{}^2\sigma_{x_i}{}^2} \tag{17}$$

Eq. (17) is the error transfer formula. In Eq. (17), σ_y is the relative error, $\alpha_i = \frac{\partial F}{\partial x_i}$ is the partial derivative of function F to independent variable x_i , σ_{x_i} is the limit measurement error of independent variable x_i. The relative error of effective thermal conductivity obtained in T- history method is ranged from 8.7% to 10.8%.

3 Results and discussion

3.1 Effect of mass ratio of different CNs on thermal conductivity

Fig. 4 shows the relationship between the thermal conductivity of PCM samples and the mass ratio of different CNs. Firstly, the thermal conductivity of S2 with the addition of 20% HDPE was almost the same as that of pure paraffin. It was proved that HDPE showed no observable effect on the thermal conductivity of paraffin. Secondly, for the Paraffin-HDPE/EG-MWCNT composite PCMs, the thermal conductivities of M1 and M5 were 0.85 W/(m·K) and 0.52 W/(m·K), respectively, which increased by 240% and 108% compared to the pure paraffin. EG showed better thermal enhancement effect than MWCNT under the same content, because the porous structure of EG is more easily interconnected than the tubular structure of MWCNT and develops more effective heat conduction network.

Comparing the EG-MWCNT-based composite PCM samples, it was found that the thermal conductivity of M4 was greater than M5 but less than M1, which means that mass ratio of EG: MWCNT = 1:1 cannot establish a good-enough connection between EG and MWCNT. The thermal conductivity of M2 was the largest, reaching 1.36 W/(m·K). It was increased by 444% compared with the pure paraffin which was the largest enhancement rate, and 60% compared with M1, respectively. This illustrated that in our case EG: MWCNT = 4:1 was the optimal mass ration. A small amount of MWCNT built a more direct heat transfer bridge between EG and paraffin, and the multi-layer sheet structure of EG and the bundle structure of MWCNT demonstrated the more effective synergistic thermal enhancement effect.

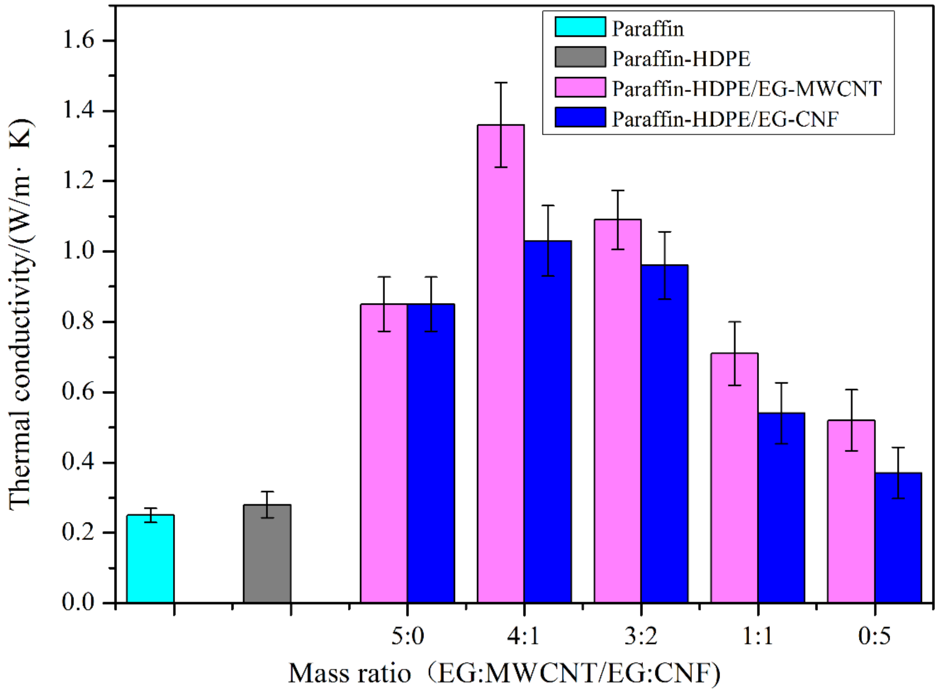

Fig. 4. Comparison of thermal conductivity of the composite PCMs

For Paraffin-HDPE/EG-CNF composite PCMs, the thermal conductivities of C1 and C5 were 0.85 W/(m·K) and 0.37 W/(m·K) respectively, which were 240% and 48% higher than the pure paraffin. It is proved that the heat conduction enhancement effect of EG is more significant than that of CNF under the same content. Comparing the EG-CNF-based composite PCMs, the thermal conductivity of C4 was between C1 and C5, indicating that mass ratio of EG: CNF = 1:1 cannot effectively establish the heat transfer connection. The thermal conductivities of C2 and C3 were higher than those of samples with other mass ratio. The thermal conductivity of C2 was the largest, reaching 1.03 W/(m·K), which increased by 312% compared with the pure paraffin and 21.2% compared with C1. Apparently the multi-layer structure of EG and the fibrous structure of CNF can establish a better heat conduction channel compared with the single EG or CNF, and the optimal synergistic thermal enhancement effect demonstrated was at the mass ratio of EG:CNF = 4:1, which can get the maximum level of thermal conductivity improvement at 5%

loading of thermal conductive fillers.

Comparing the two types of composite PCMs, the mass ratios of EG-MWCNT and EG-CNF had the same effect rule on the thermal conductivity, with EG-MWCNT-based composite PCMs showing better thermal conductivities than EG-CNF-based composite PCMs due to the higher thermal conductivity of MWCNT than CNF. Both EG-MWCNT-based and EG-CNF-based composite PCMs showed the best synergistic thermal enhancement effect at the mass ratio of 4:1, increased by 60% and 21.2% respectively compared to the case with only 5% EG. The mass ratio of 4:1 was proved to be able to establish a more effective heat conduction pathway, promoting heat transfer more quickly within the whole PCM composite. It is worth mentioning that the thermal conductivity of M3 (EG: MWCNT = 3:2) was slightly higher than that of C2 (EG: CNF = 4:1). There are two possible reasons: (1) although 4:1 is the best mass ratio of the synergistic thermal enhancement effect, the thermal conductivity of MWCNT is better than that of CNF, so a smaller ratio could perform better as the thermal conductivity of a composite PCM is the result of the superposition of two kinds of heat conduction effects; (2) EG produces interfacial thermal resistance between the structural contact surfaces in the composite materials. Relevant research showed that nano-materials can reduce the interfacial thermal resistance by reducing the phonon scattering [21]. It was speculated that MWCNT can reduce the thermal resistance of EG more effectively than CNF. This speculation will be certified in the following prediction model of thermal conductivity.

3.2 Synergistic effect analysis of two thermal conductive CN fillers

All the existing thermal conductivity prediction models are typically based on one single dispersed phase, but two different kinds of fillers as dispersed phase are not involved. In the most common prediction models for composite materials as shown in Table 1, k_c is the thermal conductivity of the composite materials; k_m is the thermal conductivity of the Paraffin-HDPE matrix; k_p is the thermal conductivity of the EG/MWCNT/CNF particle fillers; s is the area fraction, which is calculated by Eq. (10) , where l/d is the aspect ratio; V_p is the particle volume fraction and calculated by Eq. (11), where ρ_m is the density of matrix, ρ_p is the density of EG/MWCNT/CNF thermal conductive fillers, and w_p is the mass fraction of the fillers. α is defined as a dimensionless parameter indicating the thermal effect of particle dispersion in the matrix, which is determined by thermal conductivity k_p, interfacial thermal resistance R_{Bd} and dispersion radius r, calculated by

Eq. (12). The interfacial thermal resistance of CNs is generally at the magnitude of 10^{-7} m^2K/W [22].

$$s = V_p \cdot \frac{l}{d} \tag{10}$$

$$V_p = \frac{1}{1 + \left(\frac{1}{w_p} - 1\right) + \frac{\rho_p}{\rho_m}} \tag{11}$$

$$\alpha = \frac{R_{Bd} k_p}{r} \tag{12}$$

In the current paper, EG was regarded as the dispersed phase in the samples of EG: MWCNT/EG:CNF = 5:0, 4:1, 3:2 and 1:1, whilst MWCNT/CNF was regarded as the dispersed phase in the samples of EG:MWCNT/EG:CNF=0:5. After repeated calculations, when using the Bruggeman and Maxwell-Garnett models with only EG/MWCNT/CNF contained in the system, α was found to be 0.05, 0.02 and 0.035, respectively, to best fit the experimental values and conform to the thermal resistance law of the CNs. The calculated thermal resistance values of EG/MWCNT/CNF by Eq. (12) were 3.34×10^{-7} m^2K/W, 2.05×10^{-7} m^2K/W and 6.08×10^{-7} m^2K/W, respectively. The results using the five models in Table 1 to fit the tested thermal conductivity values of Paraffin-HDPE/EG-MWCNT and Paraffin-HDPE/EG-CNF are shown in Fig. 5 and Fig. 6.

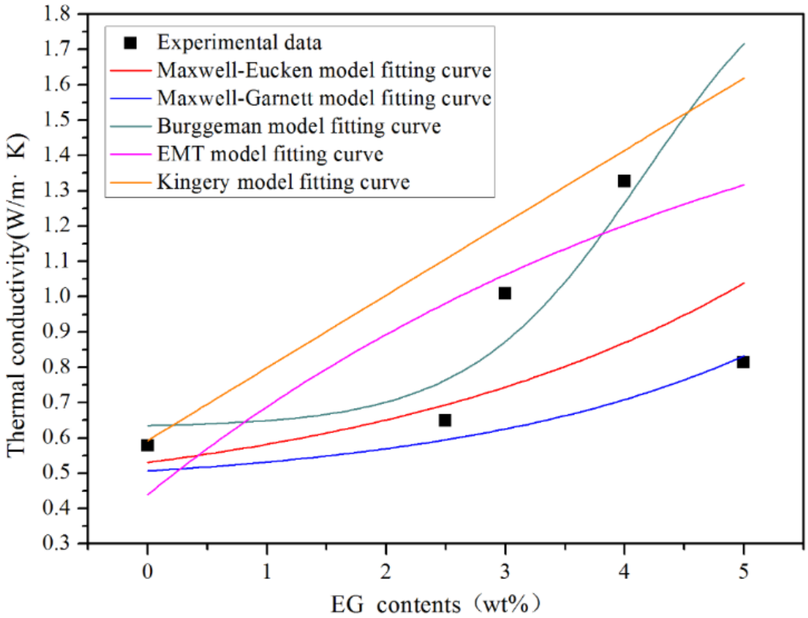

Fig. 5. Comparison between experimental and theoretical values of the Paraffin-HDPE/EG-MWCNT thermal conductivities

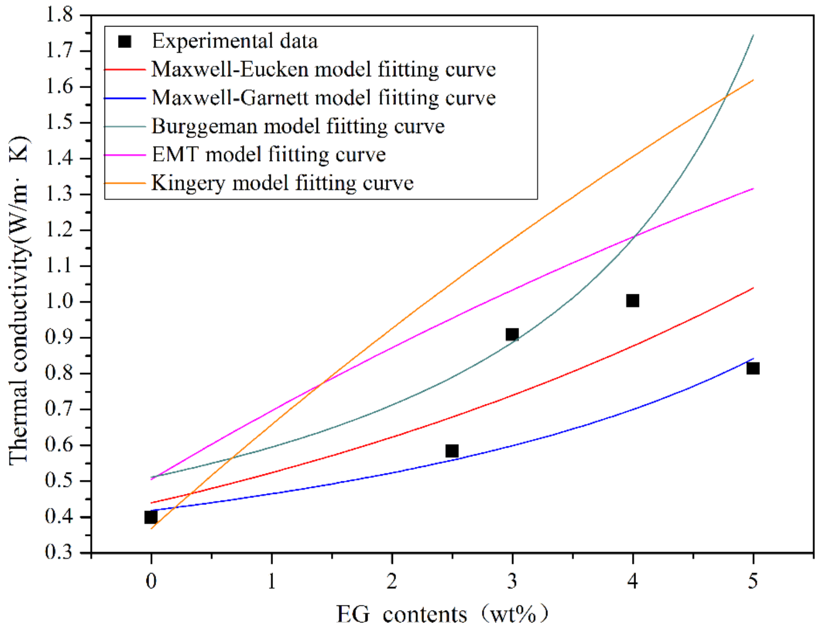

Fig. 6. Comparison between experimental and theoretical values of the Paraffin-HDPE/EG-CNF thermal conductivities

As shown in Fig. 5 and Fig. 6, for all the samples of EG:MWCNT /EG:CNF = 5:0, 4:1, 3:2 and 1:1, the calculated thermal conductivity of the composite PCM always increased with the increase of the EG content. The calculated results using the prediction model were related to the selected thermal conductive filler. For the three kinds of CNs selected in the experiment (EG/MWCNT/CNF), the agreement between the predicted values of the Maxwell-Garnett model and the experimental values was found the best at EG:MWCNT = 5:0 and 0:5 and EG:CNF = 0:5.

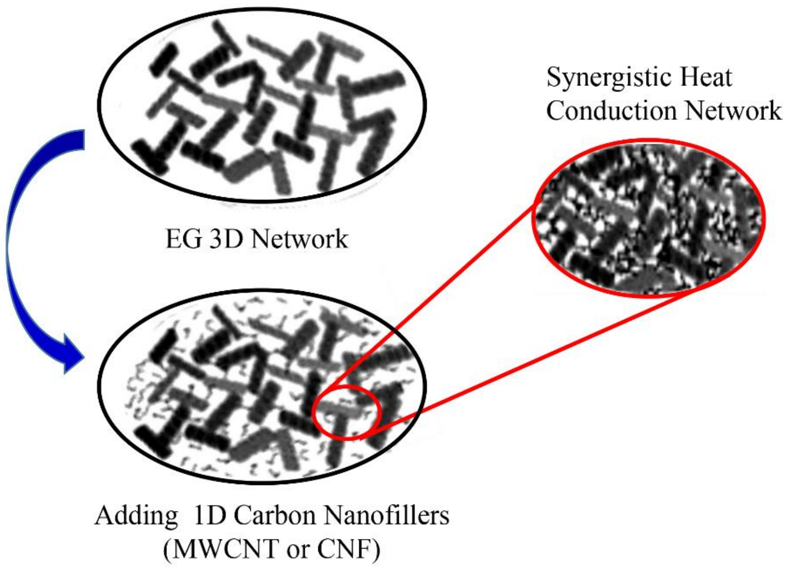

Fig. 7. Schematic diagram of synergistic thermal enhancement effect

At EG:MWCNT/EG:CNF = 4:1, 3:2, 1:1, the experimental values were higher than the theoretical values due to the synergistic thermal enhancement effect between EG and MWCNT/CNF, which can be attributed to the hybrid of MWCNT/CNF infiltrating in the EG network [23]. As shown in Fig. 7, when the content of EG was sufficient to form a heat conduction network, the "holes" in the network were very small. At this time, large pieces of worm-like structured EG cannot fill these holes, and a small amount of 1D tubular-type carbon nanofillers (MWCNT and CNF) can connect both sides of EG to fill the holes, making the heat conduction network more compact and conductive, thus producing a better heat conduction enhancement effect than the single EG.

The synergistic effect of two thermal conductive CN fillers (EG-MWCNT, EG-CNF) is represented by the synergy factor η [24], thus the Maxwell-Garnett model is modified to Eq. (13).

$$k_c = \eta \cdot \frac{\left[k_m\left(1+2\alpha\right)+2k_p\right]+2V_p\left[k_m(1-\alpha)-k_p\right]}{\left[k_m\left(1+2\alpha\right)+2k_p\right]-V_p\left[k_m(1-\alpha)-k_p\right]} \cdot k_p \tag{13}$$

After modified calculation, the synergistic factors η of EG: MWCNT = 4:1, 3:2, 1:1 were 1.8, 1.6, 1.2, respectively, and the synergistic factors η of EG: CNF = 4:1, 3:2, 1:1 were 1.4, 1.3, 1.1, respectively. Fig. 8 and Fig. 9 show the fitting results of the modified model and experimental values. The deviations between the experimental and theoretical values of Paraffin-HDPE/EG-MWCNT and Paraffin-HDPE/EG-CNF were within 1.8%-3.9% and 0.6%-3.9% respectively, exhibiting a good fitting accuracy.

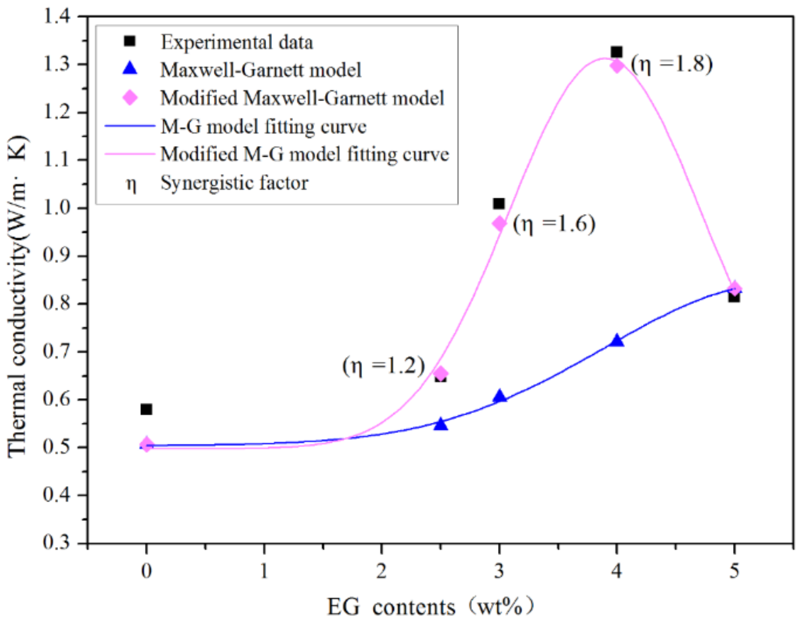

Fig. 8. Comparison of experimental values, theoretical values and correction values of Paraffin-HDPE/EG-MWCNT thermal conductivity

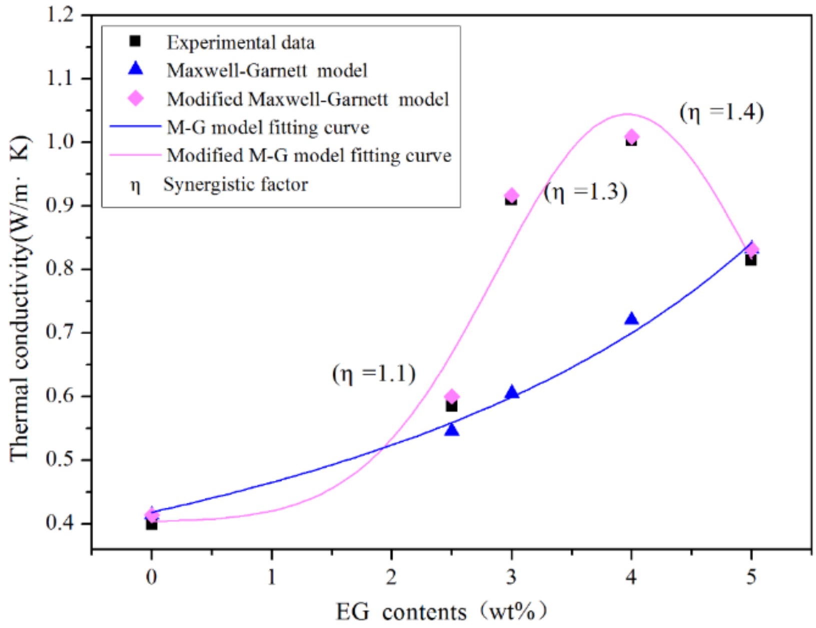

Fig. 9. Comparison of experimental values, theoretical values and correction values of Paraffin-HDPE/EG-CNF thermal conductivity

The degree of synergistic effect between the two different CNs fillers was judged by the value of the synergistic factor η, that is, EG:MWCNT = 4:1 > EG:MWCNT = 3:2 > EG:CNF = 4:1 > EG:CNF = 3:2 > EG:MWCNT = 1:1 > EG:CNF = 1:1. Such relationship is consistent with the experimental values of the thermal conductivities. The modified Maxwell-Garnett model was proved to be the most reasonable to predict the effective thermal conductivity of the Paraffin-HDPE/EG-MWCNT and Paraffin-HDPE/EG-CNF composite PCMs within the range of the mass ratio studied in this paper.

There are two possible reasons to explain why the thermal conductivities of Paraffin-HDPE/EG-MWCNT were better than those of Paraffin-HDPE/EG-CNF. Firstly, the synergy effect of EG-MWCNT is stronger than that of EG-CNF as shown in Fig. 8 and Fig. 9, thus more effective heat conduction pathway can be formed. Secondly, the system interfacial thermal resistance is different. The relationship of the interfacial thermal resistance for the three CNs obtained by Eq. (11) is $R_{Bd\_CNF} > R_{Bd\_EG} > R_{Bd\_MWCNT}$, so the Paraffin-HDPE/EG-MWCNT had the smallest interfacial thermal resistance, thereby had a relatively higher thermal conductivity. Therefore, increasing the synergy effect of the fillers and reducing the interfacial thermal resistance of the system are two effective ways to improve the thermal conductivity of the composite PCMs, which can be further investigated.

Table 4 Thermal conductivity of the composite PCMs in this work compared with that in previous literature

Sample composition	*k* /W/(m·K)	Refs
Paraffin+9% EG	2.08	[25]
Paraffin/LDPE+15% EG	1.278	[26]
Paraffin-HDPE+4.6% EG	1.10	[27]
Paraffin/LDPE+10% EG	1.02	[28]
Paraffin+7% EG	0.74	[29]
Paraffin-HDPE+16.7% EG	1.549	[30]
Paraffin-HDPE+5% EG	0.85	[21]
Stearyl alcohol/HDPE + 3% EG	0.6698	[32]
Paraffin/Expanded perlit+1% CNT	0.285	[33]
Paraffin/Expanded perlite+5.7% MWCNT	0.516	[34]
MPCM/HDPE+5% EG	0.94	[35]
MPCM/HDPE+5% Graphite powder	0.65	
Paraffin+5% MWCNT	0.34	[36]
Paraffin+5% CNF	0.31	
Paraffin+5% GNP	0.70	
Paraffin/EVA+5.8% EG/2.5% CF	2.03	[11]
Paraffin-HDPE/SBS+9% EG	0.575	[12]
Paraffin-HDPE/SBS+7%EG/3% MWCNT	0.673	
Paraffin+0.3%MWCNT+0.7%Graphene	0.87	[13]
PEG+4% GO/10% BN	0.85	[37]
PEG+4% GO/30% BN	3	
Paraffin-HDPE+4% EG/1% MWCNT	1.36	
Paraffin-HDPE+3% EG/2% MWCNT	1.09	Present work
Paraffin-HDPE+4%EG/1% CNF	1.03	

In Table 4, the enhancement effects of PCM thermal conductivity by adding CNs fillers in the current study were compared with those in previous literature. It was found that the Paraffin-HDPE/EG-MWCNT and Paraffin-HDPE/EG-CNF composite PCMs showed better competitiveness than those enhanced by a single CNs filler. Among the samples where two kinds of thermal conductive fillers were added at the same time, the EG-MWCNT-based and EG-CNF-based composite PCMs with the mass ratio of 5% exhibited the better effect of thermal conductivity enhancement.

4 Conclusion

Through the thermal conductivity experiments based on the T history method, the effects of two kinds of hybrid CNs additives (EG-MWCNT and EG-CNF) on thermal conductivity of Paraffin-HDPE SSPCM were studied.

(1) Five mass ratios of EG: MWCNT and EG: CNF = 5:0, 4:1, 3:2, 1:1, 0:5 were tested. The mass ratios of EG-MWCNT and EG-CNF exhibited the same effect rule on the thermal conductivity enhancement, that is, M2 > M3 > M1 > M4 > M5, C2 > C3 > C1 > C4 > C5. The thermal conductivity of M2 was the largest, reaching 1.36 W/(m·K) with an enhancement of 444% compared with the pure paraffin. Moreover, the EG-

MWCNT-based composite PCM showed a better thermal conductivity than the EG-CNF-based composite PCM due to the higher thermal conductivity of MWCNT than CNF.

(2) The hybrid CN fillers achieved better thermal conductivity improvement than the single CN additive due to the synergistic thermal enhancement effect. Within EG: MWCNT and EG: CNF = 5:0, 4:1, 3:2, 1:1, 0:5, both EG-MWCNT-based and EG-CNF-based composite PCMs showed the best synergistic thermal enhancement effect at the mass ratio of 4:1, with an enhancement of 60% and 21.2%, respectively, compared to the case with only 5% EG added.

(3) From the viewpoints of the synergistic thermal enhancement effect and the interfacial thermal resistance of EG-MWCNT and EG-CNF, the principle of enhancing thermal conductivity of composite PCMs was analyzed. A modified Maxwell-Garnett model with a synergy factor η was proposed, which fitted well with the experimental values. Two main reasons were revealed for the superior thermal conductivity of Paraffin-HDPE/EG-MWCNT over Paraffin-HDPE/EG-CNF. Firstly, the synergistic effect of EG-MWCNT was stronger than that of EG-CNF, leading to a more effective heat conduction pathway established. Secondly, Paraffin-HDPE/EG-MWCNT had relatively small interface thermal resistance by better reducing the phonon scattering. Increasing the synergy of hybrid fillers and reducing the interface thermal resistance of the system are two effective ways to improve the thermal conductivity of the composite PCMs, which are worthy of further studies.

Acknowledgments

This work is supported by the Natural Science Foundation of Shandong Province in China (ZR201702120003), the Fundamental Research Funds for the Central Universities (19CX02043A), National Key R&D Program of China (2017YFC0806303), the National Natural Science Foundation of China (51206189), State Key Laboratory of Heavy Oil Processing, De Montfort University through its distinguished Vice-Chancellor 2020 Programme, and the UK Science and Technology Facilities Council (STFC) through Batteries Early Career Researcher Award. The authors greatly appreciate their financial support.

References

[1] P. Sobolčiak, H. Abdelrazeq, N.G. Özerkan, M. Ouederni, Z. Nógellová, M.A.

AlMaadeed, et al., Heat transfer performance of paraffin wax based phase change materials applicable in building industry, Applied Thermal Engineering 107 (2016) 1313-1323.

[2] C. Amaral, R. Vicente, P. Marques, Phase change materials and carbon nanostructures for thermal energy storage: A literature review, Renewable and Sustainable Energy Reviews 79 (2017) 1212-1228.

[3] F. Cheng, R.L. Wen, Z.H. Huang, M.H. Fang, Y.G. Liu, X.W. Wu, et al., Preparation and analysis of lightweight wall material with expanded graphite (EG)/paraffin composites for solar energy storage, Applied Thermal Engineering 120 (2017) 107-114.

[4] Y. Cai, Y. Hu, L. Song, Preparation and flammability of high density polyethylene/paraffin/organophilic montmorillonite hybrids as a form stable phase change material, Energy Conversion and Management 48 (2007) 462-469.

[5] X. Liu, Z. Rao, Experimental study on the thermal performance of graphene and exfoliated graphite sheet for thermal energy storage phase change material, Thermochimica Acta 647 (2017) 15-21.

[6] Z.T. Yu, X. Fang, L.W. Fan, Increased thermal conductivity of liquid paraffin-based suspensions in the presence of carbon nano-additives of various sizes and shapes, Carbon 53 (3) (2013) 277-285.

[7] S.Y. Yang, W.N. Lin, Y.L. Huang, Synergetic effects of graphene platelets and carbon nanotubes on the mechanical and thermal properties of epoxy composites, Carbon 49 (3) (2011) 793-803.

[8] Y.J. Noh, S.Y. Kim, Synergistic improvement of thermal conductivity in polymer composites filled with pitch based carbon fiber and grapheme nanoplatelets, Polymer Testing 45 (2015) 132-138.

[9] J. Yu, H.K. Choi, H.S. Kim, S.Y. Kim, Synergistic effect of hybrid graphene nanoplatelet and multi-walled carbon nanotube fillers on the thermal conductivity of polymer composites and theoretical modeling of the synergistic effect, Composites: Part A 88 (2016) 79-85.

[10] Y.H. Zhao, Y.F. Zhang, S.L. Bai, High thermal conductivity of flexible polymer composites due to synergistic effect of multilayer graphene flakes and graphene foam, Composites: Part A 85 (2016) 148-155.

[11] B.Q. Tian, W.B. Yang, L.J. Luo, Synergistic enhancement of thermal conductivity for expanded graphite and carbon fiber in paraffin/EVA form-stable phase change materials, Solar Energy 127 (2016) 48-55.

[12] Z.P. Liu, R. Yang, Synergistically-Enhanced Thermal Conductivity of Shape-Stabilized Phase Change Materials by Expanded Graphite and Carbon Nanotube, Applied Sciences 7 (6) (2017) 574.

[13] D.Q. Zou, X.F. Ma, X.S. Liu, Thermal performance enhancement of composite phase change materials (PCM) using graphene and carbon nanotubes as additives for the potential application in lithium-ion power battery, International Journal of Heat and Mass Transfer 120 (2018) 33-41.

[14] W.D. Kingery, Thermal Conductivity: XIV, Conductivity of Multicomponent Systems, Journal of the American Ceramic Society 42 (12) (1959) 617-627.

[15] P. Ranut. On the effective thermal conductivity of aluminum metal foams: Review and improvement of the available empirical and analytical models, Applied Thermal Engineering 101 (2016) 496-524.

[16] D.P.H. Hasselman, L.F. Johnson, Effective Thermal Conductivity of Composites with Interfacial Thermal Barrier Resistance, Journal of Composite Materials 21 (6) (1986) 1011-1013.

[17] A.G. Every, Y. Tzou, D.P.H. Hasselman, The effect of particle size on the thermal conductivity of ZnS/diamond composites, Acta Metallurgica et Materialia 40 (1) (1992) 123-129.
[18] C.W. Nan, R. Birringer, D.R. Clarke, Effective thermal conductivity of particulate composites with interfacial thermal resistance, Journal of Applied Physics 81 (10) (1997) 6692-6699.
[19] Y.P. Zhang, J. Yi, J. Yi, A simple method, the-history method, of determining the heat of fusion, specific heat and thermal conductivity of phase-change materials, Measurement Science and Technology 10 (3) (1999) 201.
[20] Y.P. Zhang. Phase change energy storage: theory and application. Press of China University of Science and Technology, 1996.
[21] R.J. Warzoha, R.M. Weigand, A.S. Fleischer, Temperature-dependent thermal properties of a paraffin phase change material embedded with herringbone style graphite nanofibers, Applied Energy 137 (2015) 716-725.
[22] S.T. Huxtable, D.G. Cahill, S. Shenogin, Interfacial heat flow in carbon nanotube suspensions, Nature Materials 2 (11) (2003) 731-734.
[23] Z.G. Wang, F. Gong, W.C. Yu, Synergetic enhancement of thermal conductivity by constructing hybrid conductive network in the segregated polymer composites, Composites Science and Technology 162 (2018) 7-13.
[24] W. Yu, H. Xie, L. Yin, Exceptionally high thermal conductivity of thermal grease: Synergistic effects of graphene and alumina, International Journal of Thermal Sciences 91 (2015) 76-82.
[25] G. Jiang, J. Huang, Y. Fu, Thermal optimization of composite phase change material/expanded graphite for Li-ion battery thermal management, Applied Thermal Engineering 108 (2016) 1119-1125.
[26] S. Patrik, K. Mustapha, A.M. Mariam, Thermal characterization of phase change materials based on linear low-density polyethylene, paraffin wax and expanded graphite, Renewable Energy 88 (2016) 372-382.
[27] W.L. Cheng, R.M. Zhang, K. Xie, Heat conduction enhanced shape-stabilized paraffin/HDPE composite PCMs by graphite addition: Preparation and thermal properties, Solar Energy Materials and Solar Cells 94 (10) (2010) 1636-1642.
[28] I. Krupa, Z. Nógellová, Z. Špitalský, Positive influence of expanded graphite on the physical behavior of phase change materials based on linear low-density polyethylene and paraffin wax, Thermochimica Acta 614 (2015) 218-225.
[29] Z. Li, W.G. Sun, G. Wang, Experimental and numerical study on the effective thermal conductivity of paraffin/expanded graphite composite, Solar Energy Materials and Solar Cells 128 (9) (2014) 447-455.
[30] J.W. Liu, W.B. Yang, B.Q. Tian, Influence factors on the thermal conductivity of paraffin/high density polyethylene/expanded graphite heat conduction reinforced composite phase change materials, Polymer Materials Science and Engineering 31 (5) (2015) 83-86.
[31] X.L. Wang, Q.G. Guo, L.Y. Wang, Research on high heat conduction Fixed polyethylene/paraffin/expanded graphite phase change composites, Funct. Mater. 44 (23) (2013) 3401-3404. (in Chinese)
[32] Y. Tang, Y. Lin, Y. Jia, Improved thermal properties of stearyl alcohol/high density polyethylene/expanded graphite composite phase change materials for building thermal energy storage, Energy & Buildings, 2017.
[33] A. Karaipekl, A. Biçer, A, Sari, Thermal characteristics of expanded perlite/paraffin composite phase change material with enhanced thermal conductivity using carbon nanotubes, Energy Conversion and Management 134 (2017) 373-381.

[34] X. Zhang, R. Wen, Z. Huang, Enhancement of thermal conductivity by the introduction of carbon nanotubes as a filler in paraffin/expanded perlite form-stable phase-change materials, Energy & Buildings 149 (2017).
[35] X. Wang, Q. Guo, J. Wang, Thermal conductivity enhancement of form-stable phase-change composites by milling of expanded graphite, micro-capsules and polyethylene, Renewable Energy 60 (4) (2013) 506-509.
[36] L.W. Fan, X. Fang, X. Wang, Effects of various carbon nanofillers on the thermal conductivity and energy storage properties of paraffin-based nanocomposite phase change materials, Applied Energy 110 (5) (2013) 163-172.
[37] J. Yang, L.S. Tang, R.Y. Bao, Hybrid network structure of boron nitride and graphene oxide in shape-stabilized composite phase change materials with enhanced thermal conductivity and light-to-electric energy conversion capability, Solar Energy Materials and Solar Cells 174 (2018) 56-64.